INT. J. RADIAT. BIOL 2003, VOL. 79, NO. 3, 175–180

Taylor & Francis
healthsciences

Absorbed fraction of radon progeny in human bronchial airways with bifurcation geometry

D. NIKEZIC†‡, B. NOVAKOVIC‡ and K. N. YU†*

(Received 21 August 2002; accepted 8 January 2003)

Abstract.
Purpose: The absorbed fraction, defined as the portion of the initial particle energy which is absorbed in the tissue of interest, was calculated, under bifurcation geometry of the airway tubes, for alpha-particles emitted from radon progeny in the human respiratory tract. The results are given for all branching generations and compared with the data obtained for the commonly used infinite straight cylinders adopted by the International Commission on Radiological Protection (ICRP) Report 66.
Materials and methods: A model was created to calculate the absorbed fraction of alpha-particle energy in the human lung using bifurcation geometry. Monte Carlo simulations of alpha-particle propagation in tissue and air were performed. The stopping powers of alpha-particles were adopted from the International Commission of Radiation Units and Measurements (ICRU) Report 49.
Results: The absorbed fractions for the bifurcation geometry are given for the 15 generations in the tracheobronchial tree for alpha-particle energies of 6 and 7.69 MeV. The sources were assumed to be the fast and slow moving mucus.
Conclusions: Comparisons with ICRP66 data reveal that the assumption of long, straight cylinders was appropriate in some cases, but not in all. Adoption of the absorbed fractions obtained from the bifurcation model instead of the ICRP66 data caused 'redistribution' of doses in the bronchial (BB) and bronchiolar (bb) regions.

1. Introduction

Results of the calculation of the absorbed fraction (AF) of alpha-particles emitted from radon progeny in the human respiratory tract are presented. The AF was defined as the portion of the initial alpha-particle energy that is absorbed in the tissue of interest. This quantity was calculated in the ICRP66 report (ICRP 1994) and given for various combinations of sources, targets and energies in the form of tables in appendix H of the report. The model used in the calculations is presented on pp. 8–21 of the report. The geometry of the airway tube is shown on p. 11, and the cross-sections through its wall on p. 15 for the bronchial (BB) region and on p. 17 for the bronchiolar (bb) region (figures 5 and 6 of the ICRP66 report). The BB region consists of the trachea and bronchi, while the bb region consists of the bronchioles and terminal bronchioles. The dimensions, i.e. the thickness of the various layers in the airway wall, are also given in detail in these figures. The sensitivity analyses performed by Marsh and Birchall (2000) have shown that the thickness of these layers is among the most critical parameters in the dose determination; the reliability factor for the layer thickness was 1.64. The only parameter with a larger reliability factor (1.71) was the unattached fraction of radon progeny.

While the wall structure and thickness were discussed in detail, nothing was mentioned in ICRP66 about the tube length used in the calculations of AF. The dimensions of the model (including the diameters and lengths of the airway tubes, as well as the branching angle and gravity angle) of the tracheobronchial (T-B) tree in an adult male was indeed given in table 2 (p. 14) of ICRP66, but it was used for calculation of aerosol deposition and not for AF. In reality, the T-B tree should comprise a series of bifurcations (hereafter the 'bifurcation geometry') and the tube lengths should vary from one generation to another. Generations were defined as sequential bifurcations of the airways. The trachea was defined as generation 0. The BB encompassed generations 0–8 and the bb generations 9–15. The bifurcation geometry was also considered by Hofmann *et al.* (1995, 2001) when determining the enhanced deposition at the bifurcations themselves, but not for the calculation of AF. Visualization and computer simulation of tubular branching in the T-B tree were also given by Spencer *et al.* (2001).

The objectives of the present paper are as follows:

- To examine the influence of tube length on AF.
- To calculate the AF for bifurcating tubes and identify the influence of this modification on the final values of AF.

2. Model

The model used for present calculations was the same as that used by Nikezic and Yu (2002).

*Author for correspondence; e-mail: peter.yu@cityu.edu.hk
†Department of Physics and Materials Science, City University of Hong Kong, Tat Chee Avenue, Kowloon Tong, Kowloon, Hong Kong.
‡University of Kragujevac, Faculty of Science, 34000 Kragujevac, Yugoslavia.

International Journal of Radiation Biology ISSN 0955-3002 print/ISSN 1362-3095 online © 2003 Taylor & Francis Ltd
http://www.tandf.co.uk/journals
DOI: 10.1080/0955300031000085977

Therefore, it will not be elaborated in detail here. Some of the more important characteristics will be described in the following points.

- Monte Carlo simulation of alpha-particle propagation in the air–tissue system was used for AF determination.
- Stopping powers of alpha-particles in air and tissue were adopted from the ICRU49 report (1993).
- Absorbed energy, ΔE, of an alpha-particle in a particular layer was calculated as the difference between the input and output energy for that layer: $\Delta E = E_{in} - E_{out}$. In the course of simulation, all energy differences ΔE were summed up to give the total absorbed energy, E_a. The ratio of E_a to the total number, N, of simulations gave the absorbed fraction, i.e. $AF = E_a/N$.
- In all calculations, the airway wall model proposed in the ICRP66 report was adopted.

Two groups of calculations were performed. The first was related to the straight (i.e. not bifurcated) tube with a finite longitudinal dimension. Its model is shown in figure 1. The structure of the wall was omitted because it was described in the ICRP66 report. Three different alpha-particles denoted by 1, 2 and 3 with different histories are also shown. Particle 1 goes directly into the tissue; particle 2 passes through the airway cavity of the tube; particle 3 has such a direction that it will leave the system considered here. The range of alpha-particles in tissue was relatively small, and a significant part of the particles (about 46–48%) passed through air. Their range in air was of the order of a few centimetres, which is comparable with or larger than the tube length in reality, and there was a finite probability that some of them will leave the modelled tube. In the first group of our calculations, these alpha-particles were considered lost in the determination of AF.

In the second group of calculations, the bifurcation geometry shown in figure 2 was considered. The notations u, c and l mean the upper, central and lower cylinders. The lengths (h_U, h_C, h_L), diameters (d_U, d_C, d_L) and branching angles α_U and α were adopted from the ICRP66 report. The (imaginary) walls of the central cylinder are extended by halftone lines to show the difference between the straight tube and the bifurcation geometry. The numbers 1–6 again represent different alpha-particles with various histories. Particle 1 goes directly into the tissue while

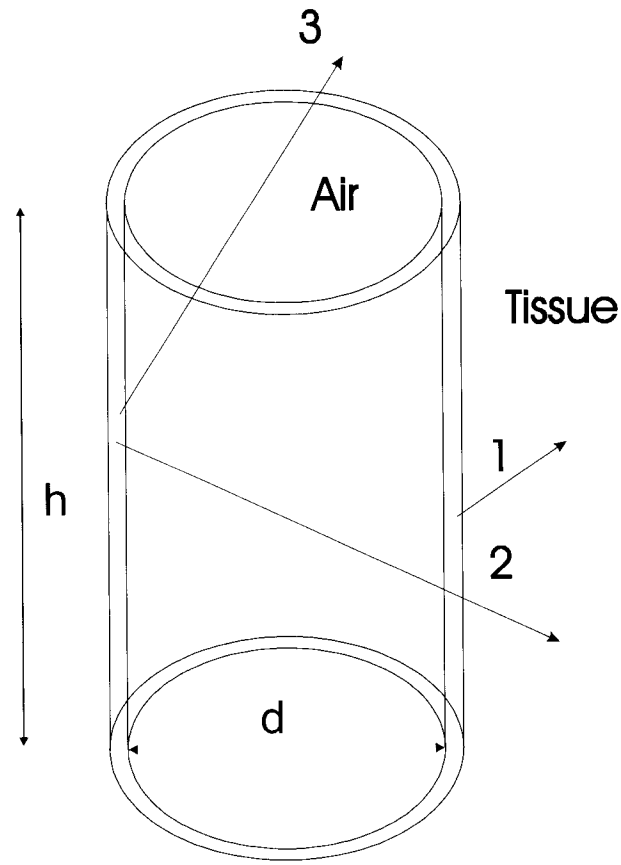

Figure 1. Model of an airway tube with an infinite length. See the text for definitions and explanations.

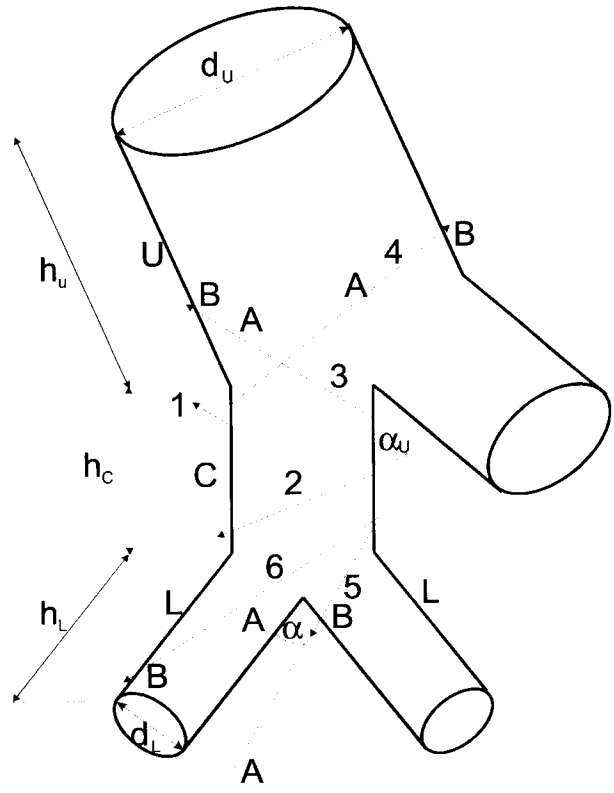

Figure 2. Bifurcation geometry of airway tubes. See the text for definitions and explanations.

particle 2 crosses the airway cavity and then strikes the opposite wall of the same cylinder; these two cases do not make any difference in comparison with the case of the straight tube. Particles 3 and 4 are emitted in the central cylinder and they go into the upper one. If the central tube is straight and long, these particles would have entered the tissue at points A (on the extended wall of the central cylinder). However, there is now a bifurcation and the particles will travel a longer distance through the air to points B where they enter the tissue. In this way, particles will lose more energy in air and enter the tissue with smaller energies. Particle 5, which is emitted in the central cylinder and goes into the lower one, will travel a shorter distance before it enters the tissue at point B. In comparison with the case of a straight cylinder, it enters the sensitive layer with a higher energy. In the BB, this sensitive layer contains target cell nuclei of secretory and basal cells. In the bb, the sensitive layer consists of nuclei of secretory cells. In contrast to particle 5, particle 6, which is travelling to the lower cylinder, will travel a much longer distance before it enters the tissue. This 'path difference' between a straight tube and the bifurcation geometry can influence AF in different ways: either to decrease or to increase it.

Note that the entrance angle becomes different when the particle 'changes' tubes, which we call here the 'angle difference'. If the entrance angle becomes larger (with respect to the normal to the surface), the particle travels a longer distance through the air and tissue before it enters the sensitive layer. In this case, the particle path through the sensitive layer is also longer, which might cause a larger deposited energy.

Nonetheless, even if the entrance energy of alpha-particles at the sensitive layer is smaller, it does not necessarily mean a smaller absorbed energy, since the stopping power and energy transfer increase with a lowering of the particle energy and they are the largest in the Bragg peak region.

All these various possibilities, as reflected in the path and angle differences, could be self-compensating when AF is calculated, but compensation might not be full. One can expect that the influence of path difference is more pronounced in larger bronchi because the path in air is longer there than in smaller airway tubes. Furthermore, the angle difference can be more important in smaller tubes where the tubes are shorter and the probability of switching from one tube to another is larger.

3. Results

3.1. *Straight cylinders*

For illustrations of the trends, the results of AF are given in figures 3 and 4, which show the variations

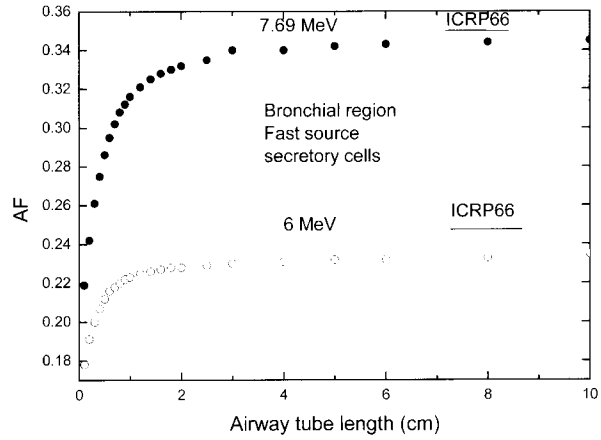

Figure 3. Absorbed fraction (AF) of alpha-particles emitted in fast-moving mucus in secretory cells of the bronchial region as a function of airway tube length. Solid circles, for 7.69 MeV alpha-particles; open circles, for 6 MeV alpha-particles. Horizontal lines labelled ICRP66 from ICRP94.

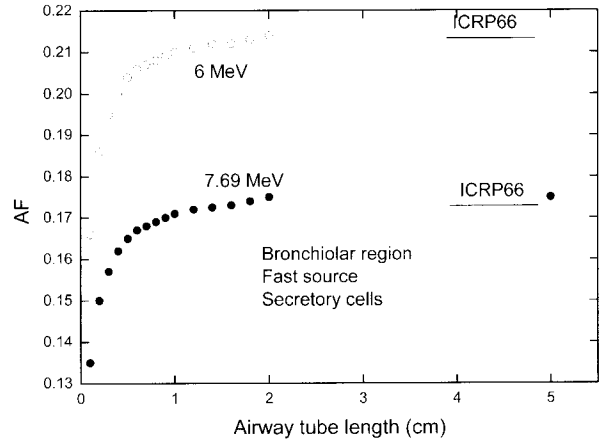

Figure 4. Absorbed fraction (AF) of alpha-particles emitted in fast-moving mucus in secretory cells of bronchiolar region as a function of airway tube length. Solid circles, for 7.69 MeV alpha-particles; open circles, for 6 MeV alpha-particles. Horizontal lines labelled ICRP66 from ICRP94.

of AF with the tube length, assuming a finite length. In both cases, the alpha source was in the fast moving mucus (fast clearing region, F). AF was calculated for secretory cells. Figure 3 is related to the BB region, while figure 4 is related to the bb region. The values given in ICRP66 (which are not related to any specific length) are also shown as horizontal lines in figures 3 and 4 (labelled ICRP66). All the curves increase with the tube length, which is expected because the fraction of particle loss at the tube ends decreases (and thus AF increases) with the tube length. Note that the curve for 7.69 MeV is above that for 6 MeV in BB, but the opposite is true in bb. All the curves saturate at large tube lengths. The

saturations obtained by our program were close to the ICRP values, being a little bit smaller in BB and a little larger in bb than the corresponding ICRP values. From these results, it is concluded that the ICRP66 calculations were performed for infinitely long airway tubes. As the figures are for illustration purposes only, the results for the slow clearing source (S) are not given.

Calculations were performed for very long tubes and the results were compared with the ICRP66 data in table 1. The agreements were better than 6%, except for the case where basal cells were irradiated by the fast mucus source. In some cases, the agreement was better than 1%. All data for the bb region obtained by our program were slightly larger than the ICRP66 data.

In reality, however, the lengths of the airway tubes were finite. In fact, the realistic geometry for the human lung consists of bifurcations. The aim here is to examine the influence of this bifurcation geometry on the AF of alpha-particles emitted in the lung. The good agreement between our results and the ICRP66 data shown above has justified the use of our program in the study of more complex geometries.

3.2. *Bifurcation geometry*

The AFs were further calculated for the bifurcation geometry. Emission points of alpha-particles were sampled uniformly in the source, but *only* in the central cylinder. The lengths, diameters and branching angles for the cylinders were taken from the ICRP66 report (p. 14) and are shown in table 2. The results for secretory cells in the BB region (generations 1–8) are shown in figure 5. For the sake of comparison, the ICRP66 data are given as horizontal lines. Four groups of data are shown: for energies 6 and 7.69 MeV, and for fast (F) and slow (S) sources.

Table 1. Comparison of the AF between the present calculations and the ICRP66 data for straight, long cylinders.

		Secretory cells		Basal cells	
Source	Method	6 MeV	7.69 MeV	6 MeV	7.69 MeV
Bronchial region (BB)					
Fast	ICRP66	0.249	0.353	5×10^{-3}	0.0893
mucus	this work	0.236	0.350	3.55×10^{-3}	0.0802
Slow	ICRP66	0.272	0.355	0.021	0.0857
mucus	this work	0.267	0.353	0.020	0.0789
Bronchiolar region (bb)					
Fast	ICRP66	0.214	0.172		
mucus	this work	0.216	0.175		
Slow	ICRP66	0.217	0.173		
mucus	this work	0.221	0.178		

Table 2. Model used in calculations (the table as given in ICRP66, p. 14).

Region	Generation	Diameter (cm)	Length (cm)	Branch angle (degrees)
BB	0	1.65	9.1	0
	1	1.20	3.8	36
	2	0.85	1.5	35
	3	0.61	0.83	28
	4	0.44	0.90	35
	5	0.36	0.81	39
	6	0.29	0.66	34
	7	0.24	0.60	48
	8	0.20	0.53	53
bb	9	0.1651	0.4367	54
	10	0.1348	0.3620	51
	11	0.1092	0.3009	46
	12	0.0882	0.2500	47
	13	0.0720	0.2069	48
	14	0.0603	0.1700	52
	15	0.0533	0.1380	45

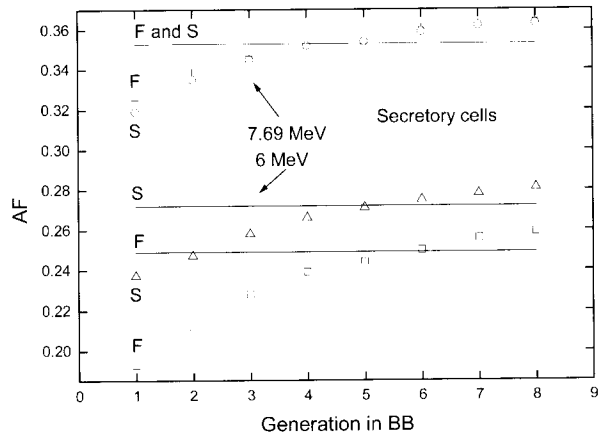

Figure 5. Absorbed fraction in secretory cells in the bronchial region (BB) (generations 1–8). The horizontal lines represent the ICRP66 data for the fast- and slow-clearance mucus for 6 and 7.69 MeV alpha-particles, respectively. The two lines for 7.69 MeV overlap with each other and are indiscernible. The scattered points represent results from the present work: □, for fast-clearance mucus and 6 MeV alpha-particles; △, for slow-clearance mucus and 6 MeV alpha-particles; ○, for slow-clearance mucus and 7.69 MeV alpha-particles; +, for fast-clearance mucus and 7.69 MeV alpha-particles.

Note that AF increases with the generation number, despite decreases in the tube lengths, contrary to the prediction using figures 3 and 4. As the diameters of the tubes decrease, the path lengths through the air become smaller, so the effect of path difference diminishes.

The AFs for 6 MeV alpha-particles are shown as the lower group of data in figure 5. For the first few generations (1–4), the AFs were well below the ICRP66 values. This difference is about 25% for

generation 1 (main bronchi). For generations 5 and 6 they were close to each other, while for generations 7 and 8 the AFs were slightly larger than the ICRP66 values. The AFs for 7.69 MeV alpha-particles are shown as the upper group of data in figure 5, which are always larger than those data for 6 MeV alpha-particles. The ICRP66 values for F and S sources were close to or overlapped with each other, so they are represented by one line. The data obtained for the bifurcation geometry were again significantly smaller than the ICRP66 values for generations 1 and 2, getting closer for generations 3–5, and becoming somewhat larger for generations 7–9.

In the ICRP66 approach, the mean dose in BB (as well as in other regions) was used. Such an approach did not give any information about the dose for a particular generation of the T-B tree. Figure 5 shows that the doses in secretory cells in generations 1–4 could be smaller by up to 25% than the average dose obtained from the ICRP66 model. For generations 7 and 8, the doses were a few per cent larger than the ICRP66 predictions.

The data for basal cells are given in figure 6. Again, four groups of data (for 6.00 and 7.69 MeV, and for F and S sources) are shown. The data for 6 MeV were consistently below the ICRP66 values for all generations. Our model gave significantly smaller AFs in basal cells for infinitely long tubes for 6 MeV incident energy from the F source. The basal cell layer begins at 46 μm below the top of the mucus and the range of 6 MeV alpha-particles in tissue was about 47 μm. These cells are at the end of the range of the alpha-particles, so the calculated dose was very sensitive to the assumed stopping power and the model. However, this value was rather small compared with other AFs and its influence on the total dose was almost negligible. Note that the AFs for 6 MeV were independent of the generation number. This is expected since an alpha-particle having crossed the air cavity in the bronchi will lose its energy before reaching the basal layer.

The AFs in basal cells from 7.69 MeV alpha-particles depend on the generation number and have trends similar to those for secretory cells. The AFs for the F source were smaller in the first three generations than ICRP66 values and become larger for the rest. However, the AFs for the S source were smaller than the ICRP66 values in the entire BB region. Therefore, adoption of AFs derived from the bifurcation geometry will give smaller doses in basal cells than the ICRP66 estimation.

Figure 7 gives the results for the bb region (generations 9–15), where only secretory cells were considered sensitive to alpha radiation. The ICRP66 data were again given as horizontal lines, while the data for the bifurcation geometry are shown as scattered points. The results for the F source (for both energies) under the bifurcation geometry were very close to or slightly larger than the ICRP66 data. However, the results for the S source were significantly higher than the ICRP66 data, and the difference also grew with

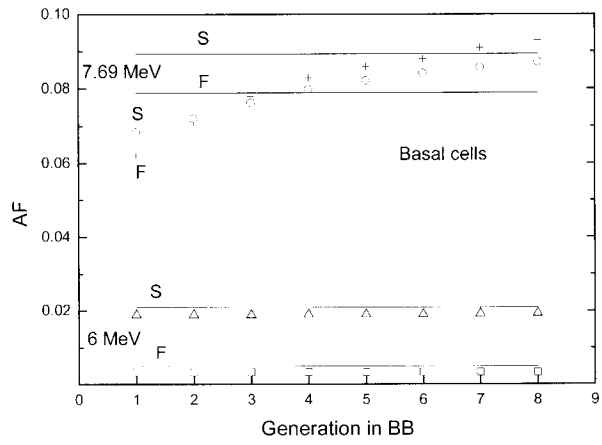

Figure 6. Absorbed fraction in basal cells in the bronchial region (BB) (generations 1–8). The horizontal lines represent the ICRP66 data for the fast- and slow-clearance mucus for 6 and 7.69 MeV alpha-particles, respectively. The scattered points represent results from the present work: □, for fast-clearance mucus and 6 MeV alpha-particles; △, for slow-clearance mucus and 6 MeV alpha-particles; ○, for slow-clearance mucus and 7.69 MeV alpha-particles; +, for fast-clearance mucus and 7.69 MeV alpha-particles.

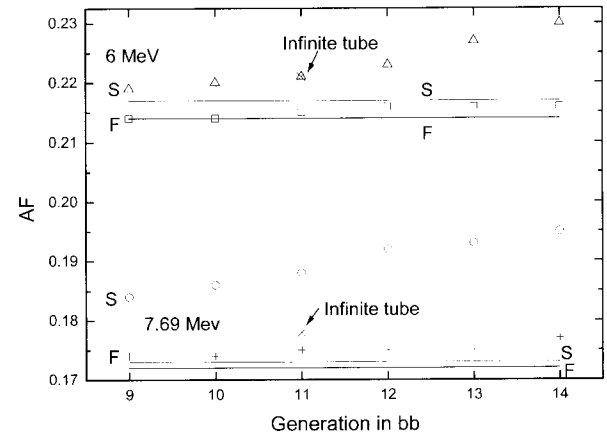

Figure 7. Absorbed fraction in secretory cells in the bronchiolar region (bb) (generations 9–15). The horizontal lines represent the ICRP66 data for the fast- and slow-clearance mucus for 6 and 7.69 MeV alpha-particles, respectively. The scattered points represent results from the present work: □, for fast-clearance mucus and 6 MeV alpha-particles; △, for slow-clearance mucus and 6 MeV alpha-particles; ○, for slow-clearance mucus and 7.69 MeV alpha-particles; +, for fast-clearance mucus and 7.69 MeV alpha-particles; ×, for infinitely long tubes and for slow source (the same as in table 1).

the generation number. For the 14th generation, the difference was about 12% for 7.69 MeV alpha-particles. In the same figure, the data obtained from our computational program for an infinitely long tube and the S source (the same result as in table 1) were marked by a cross (x). The diameter of the 11th generation was the one closest to 1 mm, which was used by ICRP66 as the most representative diameter of airway tubes in the bb region. Our value for an infinitely long tube was slightly higher than the ICRP66 value, but the results from the bifurcation geometry and the S source were much larger and cannot be explained by the difference in the program used. Therefore, adoption of AFs derived from the bifurcation geometry instead of the ICRP66 data will result in a larger dose in the bb region.

4. Conclusions

The AFs of alpha-particles in the human respiratory tract have been calculated previously in the ICRP66 report by assuming an infinite length for the airway tubes and with the most representative diameters of 5 mm in BB and 1 mm in bb. A more realistic bifurcation geometry with the dimensions given in ICRP66 has been considered here. Two regions of the T-B tree, BB and bb, were considered separately.

AF was smaller in the first few generations of BB if the bifurcation geometry was considered instead of long, straight cylinders. However, for larger generation numbers in BB, the bifurcation geometry gave slightly larger values. After a 'weighting' of the data obtained from the bifurcation model, e.g. according to the total surface area in the generations, one can get AF values very close to the ICRP66 values. In this sense, the approximation of a very long tube with the most representative diameter seems appropriate for secretory cells in the BB region.

However, in the bb region, we found systematic divergence between the two models if the S source was considered. In this case, the ICRP66 approximation was not appropriate for AF calculations.

Acknowledgement

Research was supported by a CERG grant CityU1004/99P from the Research Grant Council of Hong Kong.

References

Hofmann, W., Balashazy, I. and Heistracher, T., 2001, The relationship between secondary flows and particle deposition patterns in airway bifurcations. *Aerosol Science and Technology*, **35,** 958–968.

Hofmann, W., Balashazy, I. and Koblinger, L., 1995, The effect of gravity on particle deposition patterns in bronchial airway bifurcations. *Journal of Aerosol Science*, **26,** 1161–1168.

ICRP, 1994, *Human Respiratory Tract Model for Radiological Protection*. Report of a Task Group of the International Commission on Radiological Protection (ICRP) Publication 66 (New York: Annals of the International Commission on Radiological Protection/Pergamon), 24, 1–459.

ICRU, 1993, *Stopping Powers and Ranges for Protons and Alpha Particles*. Report 49 (Bethesda, Maryland: International Commission of Radiation Units and Measurements).

Marsh, J. W. and Birchall, A., 2000, Sensitivity analysis of the weighted equivalent lung dose per unit exposure from radon progeny. *Radiation Protection Dosimetry*, **87,** 167–178.

Nikezic, D. and Yu, K. N., 2002, Distributions of specific energy in sensitive layers of the human respiratory tract. *Radiation Research*, **157,** 92–98.

Spencer, R. M., Schroeter, J. D. and Martonen, T. B., 2001, Computer simulations of lung airway structures using data-driven surface modeling techniques. *Computers in Biology and Medicine*, **31,** 499–511.